

Polymer Chemistry

Accepted Manuscript



This is an *Accepted Manuscript*, which has been through the Royal Society of Chemistry peer review process and has been accepted for publication.

Accepted Manuscripts are published online shortly after acceptance, before technical editing, formatting and proof reading. Using this free service, authors can make their results available to the community, in citable form, before we publish the edited article. We will replace this *Accepted Manuscript* with the edited and formatted *Advance Article* as soon as it is available.

You can find more information about *Accepted Manuscripts* in the [Information for Authors](#).

Please note that technical editing may introduce minor changes to the text and/or graphics, which may alter content. The journal's standard [Terms & Conditions](#) and the [Ethical guidelines](#) still apply. In no event shall the Royal Society of Chemistry be held responsible for any errors or omissions in this *Accepted Manuscript* or any consequences arising from the use of any information it contains.

ARTICLE

Synthesis and Characterization of Branched Fullerene-terminated Poly(ethylene glycol)s

Cite this: DOI: 10.1039/x0xx00000x

Hin Chun Yau,^{a†} Mustafa K. Bayazit,^{b†} Piers R. J. Gaffney,^c Andrew G. Livingston,^c Joachim H. G. Steinke^a and Milo S. P. Shaffer^{a*}

Received 00th January 2012,
Accepted 00th January 2012

DOI: 10.1039/x0xx00000x

www.rsc.org/

Poly(ethylene glycol) [**1**, PEG_{n-4}(OH)₂, $M_n \sim 200$], glycerol ethoxylate [**2**, PEG_{n-21}(OH)₃, $M_n \sim 1000$] and pentaerythritol ethoxylate [**3**, PEG_{n-15}(OH)₄, $M_n \sim 797$] react directly with phenyl-C₆₁-butyric acid methyl ester (PCBM), in the presence of dibutyltin oxide (DBTO) catalyst at 140°C, to give a mixture of fullerene [C₆₀] end-capped PEGs via transesterification. Among these PEG linkers, only PEG_{n-4}(OPCB)₂ (**4a**) (OPCB: ester oxygen linked phenyl-C₆₁-butyryl group) was successfully isolated from the crude product mixture in the fully end-capped form. Fully acylated PEG_{n-21}(OPCB)₃ (**5**) and PEG_{n-15}(OPCB)₄ (**6**) could not be separated chromatographically from incompletely reacted species due to the polydispersity in branch lengths. This purification challenge was overcome by using a monodisperse branched core, 1,3,5-tris(octagoloxymethyl)benzene [**7**, PEG₂₄(OH)₃] to give a monodisperse tris-fullerene homostar, PEG₂₄(OPCB)₃ (**8**). The structures of the bis- and tris-fullerene products were confirmed by MALDI-TOF mass spectrometry and ¹H NMR spectroscopy with supporting FTIR and UV-vis spectroscopic analysis.

Introduction

Due to its unique optoelectronic properties, and phase behaviour, fullerene[C₆₀] is one of the most commonly used materials in the preparation of polymer donor-acceptor bulk heterojunction (BHJ) solar cells.^{1,4} However, the low solubility and processability of fullerenes in organic solvents has limited their direct use in solution and encouraged the development of a wide range of functionalised derivatives, including methanofullerenes⁵⁻⁹ and fulleropyrrolidines.^{10, 11} These functionalised derivatives offer significant increases in solubility and processability while preserving the important electronic and optical properties of the parent fullerenes. Direct functionalization of fullerenes is a simple option to prepare derivatives; however, multiple addition may occur which can affect optoelectronic properties. Phenyl-C₆₁-butyric-acid-methyl-ester (PCBM) has received considerable attention in solution-processed organic electronic applications, particularly for electron transport in solar cells.¹² As a result, this material is readily available commercially, and offers a convenient reagent for the preparation of monofunctionalized fullerene derivatives via transesterification of its methyl ester functional group.^{8, 13, 14} The performance of fullerene-polymer based bulk heterojunction (BHJ) solar cells depends on the characteristic length-scale and crystallinity of the thin, phase-segregated semiconductor active layer;¹⁵⁻¹⁹ this structure is controlled by the dynamics of the segregation process during deposition and annealing,²⁰ and by the intermolecular forces between polymer and fullerene derivatives.¹⁶ Recent studies have examined

means to modify these interfacial interactions. In particular, the use of poly(ethylene glycol) (PEG),²¹ or PEG grafted PCBM^{22, 23}, have been explored as additives to control the nano- and microstructure of the active layer, and so to produce highly stable and efficient polymer solar cells. Jeng *et al.* recently established the role of poly(ethylene glycol) dimethyl ether as an electrode buffer for the fabrication of high performance (poly-3-hexylthiophene, P3HT):PCBM based organic photovoltaics (OPVs).²² PEG-C₆₀ adducts have been variously proposed as nucleants for the fullerene rich electron transporting phase,²³ as a means to assemble an active dipole at the electrode interface,²¹ and as an encapsulant against oxidation.²³ However, the uses of short chain, multi-fullerene end-capped linear or branched PEGs, or mixtures thereof, have not yet been explored in this context. Such multiply-bound fullerenes may offer additional opportunities to enhance device performance, potentially acting as more effective nucleants, inherently bringing together groups of fullerenes. At the same time, reducing the proportion of hygroscopic PEG should decrease the sensitivity of the device to moisture. Synthetically, the preparation of multi-fullerene end-capped PEG dumbbells and stars has already been addressed via azide chemistry.^{24, 25} However, these reactions with fullerenes do not yield pure mono-substituted adducts.²⁶ The possible addition of more than one PEG-azide to a single fullerene creates a mixture of large molecules that is hard to separate. The one-step transesterification of PCBM provides a simple alternative that has not yet been exploited for the preparation of multi-fullerene end-capped PEGs. To date, the mono-fullerene end-capped

PEG chains used in BHI studies have had polymer weights of 2000–4000 Da. The large number of hygroscopic ethylene oxide repeat units per fullerene (*ca.* one C₆₀ per 45–90 monomers) makes the devices highly moisture sensitive.^{21–23} Finally, in order to improve control during the BHI phase segregation, it would be desirable to use pure, monodisperse PEG-PCBM materials as it is anticipated that these will enhance the self-assembly of ordered, well-defined structures.²⁷ The present study develops a synthetic protocol for the preparation of multi-fullerene, end-capped polydisperse linear PEGs, and three- and four-arm PEG stars. Several challenges were encountered during isolation of fully fullerene end-capped PEGs. These difficulties were addressed by the preparation of a monodisperse multi-fullerene end-capped three-arm PEG homostar. Traditionally, such PCBM derivatives have been synthesised by first hydrolysing the methyl ester into carboxylic acid to give [6,6]-phenyl-C₆₁-butyric acid (PCBA), and then converting to the acid chloride for further condensation.²⁸ However, the carboxylic acid derivative (PCBA) is only sparingly soluble in organic solvent (*ortho*-dichlorobenzene or carbon disulphide) which limits large scale synthesis. Instead, in this paper, the multi-fullerene stars were prepared via a single step catalytic transesterification with dibutyltin oxide (DBTO).²⁹ This approach avoids the multistep synthetic route and more importantly, the low solubility of PCBA during the synthesis.

Experimental

Materials and Methods

Poly(ethylene glycol) [**1**, PEG₄(OH)₂, average molecular weight, $M_n \sim 200$], glycerol ethoxylate [**2**, PEG₂₁(OH)₃, average $M_n \sim 1000$], pentaerythritol ethoxylate [**3**, PEG₁₅(OH)₄, average $M_n \sim 797$] were bought from *Sigma-Aldrich* and azeotropically dried by evaporation from anhydrous acetonitrile, 99.8%, *Sigma-Aldrich* prior to use. 1,3,5-tris(octagoloxymethyl)benzene [**7**, PEG₂₄(OH)₃] was synthesized according to the procedure recently reported and similarly azeotropically dried.³⁰ Dibutyltin oxide (DBTO, 98%, *Sigma-Aldrich*) was dried at 200°C *in vacuo* for 30 min prior to use. Phenyl-C₆₁-butyric acid methyl ester (PCBM, >99%, *Solenne BV*) was dried under vacuum at room temperature prior to use. Silica gel for column chromatography [Geduran® Si 60 (40–63µm), *Merck*] was neutralised using sodium bicarbonate (*VWR*).

Trans-2-[3-(4-*tert*-butylphenyl)-2-methyl-2-propenylidene]malononitrile (DCTB) (>98%, *Sigma-Aldrich*) and sodium iodide (99.999%, *Sigma-Aldrich*) were used as the matrix for MALDI-TOF mass spectrometry. *ortho*-Dichlorobenzene (*o*-DCB) (anhydrous, >99.8%, *Sigma-Aldrich*), trifluoroacetic anhydride (TFAA) (≥99.8%, *Sigma-Aldrich*), thin layer chromatography plates (TLC Silica gel 60 F₂₅₄, *Merck*), toluene, tetrahydrofuran and methanol (HPLC grade, *VWR*) were purchased and used as received.

Characterization

Mass spectrometry

Matrix-assisted laser desorption ionization time-of-flight (MALDI-TOF) mass spectral data were acquired on a *Waters* MICROMASS® MALDI micro MX™ with a nitrogen laser at 333 nm (power range from 150–220 mW), in the positive reflectron mode with delayed extraction. Analytical samples (1–2 mg) dissolved in toluene (10 µL) were added to a mixture of DCTB matrix in THF (10 mg mL⁻¹, 10 µL) and NaI in THF

(3 mg mL⁻¹, 3 µL). A small aliquot of this mixture (3 µL) was loaded onto a cold stainless steel target plate and allowed to air dry at room temperature. The instrument was calibrated in the range of 500–5000 Da using a poly(ethylene glycol) standard. The simulated isotopic peak patterns were constructed using online software MoIE - Molecular Mass Calculator v2.02 (ma-mdb.cas.albany.edu/RNAmods/masspec/mole.htm).

NMR spectroscopy

NMR spectra were acquired using a *Bruker* AM 400 spectrometer operating at 9.4T. Samples were dissolved in CDCl₃ and all spectra were recorded with 16 scans and $D_1 = 1$ sec. All chemical shifts (δ) are given in ppm, where the residual CHCl₃ peak was used as an internal reference for ¹H NMR ($\delta_H = 7.28$ ppm), and the CDCl₃ peak for ¹³C NMR ($\delta_C = 78.23$ ppm). Coupling constants (J) are given in Hz, and chemical splitting patterns are abbreviated as follows: s, singlet; d, doublet; t, triplet; q, quartet; quin, quintet and m, multiplet.

UV-vis Spectroscopy

UV-visible spectra were collected using a *Perkin-Elmer* Lambda 950 spectrophotometer. Samples were dissolved in toluene and spectra were recorded from 200 to 800 nm with a resolution of 1 nm, using a 1.0 cm UV quartz cuvette.

FTIR Spectroscopy

Fourier transform infrared spectra were recorded on powders using a *Perkin-Elmer* spectrometer 100 equipped with a Pike attenuated total reflectance (ATR) silicon crystal.

General procedure for synthesis of fullerene end-capped PEGs.

PCBM [1.1 eq. for each PEG(OH)_n hydroxyl group] was dissolved in *o*-DCB (10 mL) under N₂ at room temperature, and added to PEG and DBTO [0.11 eq. for each PEG(OH)_n hydroxyl group] in a two-necked round-bottomed flask. The solution was then heated at 140°C for 5 days under N₂, after which the solvent was evaporated under a stream of N₂ at room temperature, and the resulting dark brown residue fractionated by silica gel column chromatography. Unreacted PCBM eluted with toluene, after which fractions were collected eluting with toluene-methanol (9:1 v/v). Depending on their purity, as determined by ¹H NMR, the fractions were further purified, either by additional column chromatography and/or preparative TLC until ¹H NMR the integral of the peaks remained constant upon further purification.

Synthesis of PEG₄(OPCB)₂, **4**.

Polydisperse bis-C₆₀ linear PEG **4** was synthesized from PEG₄(OH)₂ (**1**, 30 mg, 0.14 mmol), PCBM (280 mg, 0.31 mmol) and DBTO (8 mg, 0.03 mmol) using the general method described above, and fractionated through a single silica gel column, eluting with toluene-methanol (9/1 v/v), to give PEG₄(OPCB)₂ (**4**, 25 mg, 9 %) as a brown solid. R_f toluene-methanol (9:1 v/v) 0.43; δ_H (400 MHz, CDCl₃) 2.20 (quin, $J = 7.6$ Hz, 4H), 2.57 (t, $J = 7.3$ Hz, 4H), 2.93 (t, $J = 8.1$ Hz, 4H), 3.60–3.77 (m, 17H), 4.25 (t, $J = 4.3$ Hz, 4H), 7.49 (t, $J = 7.5$ Hz, 2H), 7.56 (t, $J = 7.6$ Hz, 4H), 7.93 (d, $J = 7.9$ Hz, 4H) ppm; ν (FT-IR; ATR) 2917 (aliphatic C-H stretching), 2855 (aliphatic C-H stretching), 1732 (carbonyl stretching of PCBM

ester), 1599, 1562, 1493, 1374, 1021 (**C-O** symmetric stretching of PEG), 797, 755, 695 cm^{-1} ; λ (UV-vis; toluene) 330, 433, 510 nm; m/z (MALDI-TOF) calc'd for $[\text{C}_{152}\text{H}_{42}\text{O}_8\text{Na}]^+$ 2017.23 m/z , found $[\text{M}+\text{Na}]^+$ 2017.21 m/z .

Synthesis of mixture of PEG₋₂₁(OPCB)₃, **5a**, and PEG₋₂₁(OPCB)₂(OH), **5b**.

Polydisperse tris-C₆₀ 3-arm branched PEG **5a** was synthesized from PEG₋₂₁(OH)₃ (**2**, 50 mg, 0.05 mmol), PCBM (150 mg, 0.16 mmol) and DBTO (4 mg, 0.01 mmol) using the general method described above, and fractionated through silica gel columns (2 ×), followed by preparative TLC (3 ×), eluting with toluene-methanol (9:1 v/v), to give a mixture of PEG₋₂₁(OPCB)₃ (**5a**) and PEG₋₂₁(OPCB)₂(OH) (**5b**) (40 mg, 22 %, **5a:5b** ca. 1:9 by ¹H NMR integration) as a brown solid. R_f toluene-methanol (9:1 v/v) 0.30; δ_{H} (400 MHz, CDCl₃) 2.08 (s, 5 H), 2.20 (quin, $J = 7.8$ Hz, 4.4H), 2.57 (t, $J = 7.5$ Hz, 4.4H), 2.91 (t, $J = 8.1$ Hz, 4.4H), 3.47-3.85 (m, 84.6H), 4.25 (t, $J = 4.3$ Hz, 4.4H), 7.49 (t, $J = 7.5$ Hz, 2.2H), 7.57 (t, $J = 7.6$ Hz, 4.4H), 7.94 (d, $J = 7.9$ Hz, 4.4H) ppm; ν (FT-IR; ATR) 2912 (aliphatic **C-H** stretching), 2862 (aliphatic **C-H** stretching), 1731 (carbonyl stretching of PCBM ester), 1600, 1446, 1428 (**C=C** stretching in fullerene), 1348, 1294, 1247, 1095 (**C-O** symmetric stretching of PEG), 944, 848, 755, 699 cm^{-1} ; λ (UV-vis; toluene) 330, 433, 510 nm; m/z (MALDI-TOF) calc'd for $[\text{C}_{256}\text{H}_{118}\text{O}_{26}\text{Na}]^+$ 3629.78 m/z , found $[\text{M}+\text{Na}]^+$ 3627.87 m/z .

Synthesis of mixture of PEG₋₁₅(OPCB)₄, **6a**, and PEG₋₁₅(OPCB)₃(OH), **6b**.

Polydisperse tetrakis-C₆₀ 4-arm branched PEG **6** was synthesized from PEG₋₁₅(OH)₄ (**3**, 40 mg, 0.05 mmol), PCBM (200 mg, 0.22 mmol) and DBTO (5 mg, 0.02 mmol) using the general method described above, and fractionated through silica gel columns (2 ×), followed by preparative TLC (3 ×), eluting with toluene-methanol (9:1 v/v), to give a mixture of PEG₋₁₅(OPCB)₄ (**6a**) and PEG₋₁₅(OPCB)₃(OH) (**6b**) (35 mg, 16 %, **6a:6b** ca. 1:1 by ¹H NMR integration) as a brown solid. R_f toluene-methanol (9:1 v/v) 0.32; δ_{H} (400 MHz, CDCl₃) 2.21 (quin, $J = 7.7$ Hz, 8.1H), 2.58 (t, $J = 7.5$ Hz, 8.1H), 2.94 (t, $J = 8.1$ Hz, 8.1H), 3.45 (s, 5.4H), 3.53-3.67 (m, 61.2H), 4.26 (t, $J = 4.3$ Hz, 7.5H), 7.50 (t, $J = 7.5$ Hz, 4.1H), 7.58 (t, $J = 7.6$ Hz, 8.1H), 7.95 (d, $J = 7.9$ Hz, 8.1H); ν (FT-IR; ATR) 2924 (aliphatic **C-H** stretching), 2862 (aliphatic **C-H** stretching), 1731 (carbonyl stretching of PCBM ester), 1602, 1423 (**C=C** stretching in fullerene), 1242, 1093 (**C-O** symmetric stretching of PEG), 952, 796, 755, 700 cm^{-1} ; λ (UV-vis; toluene) 330,

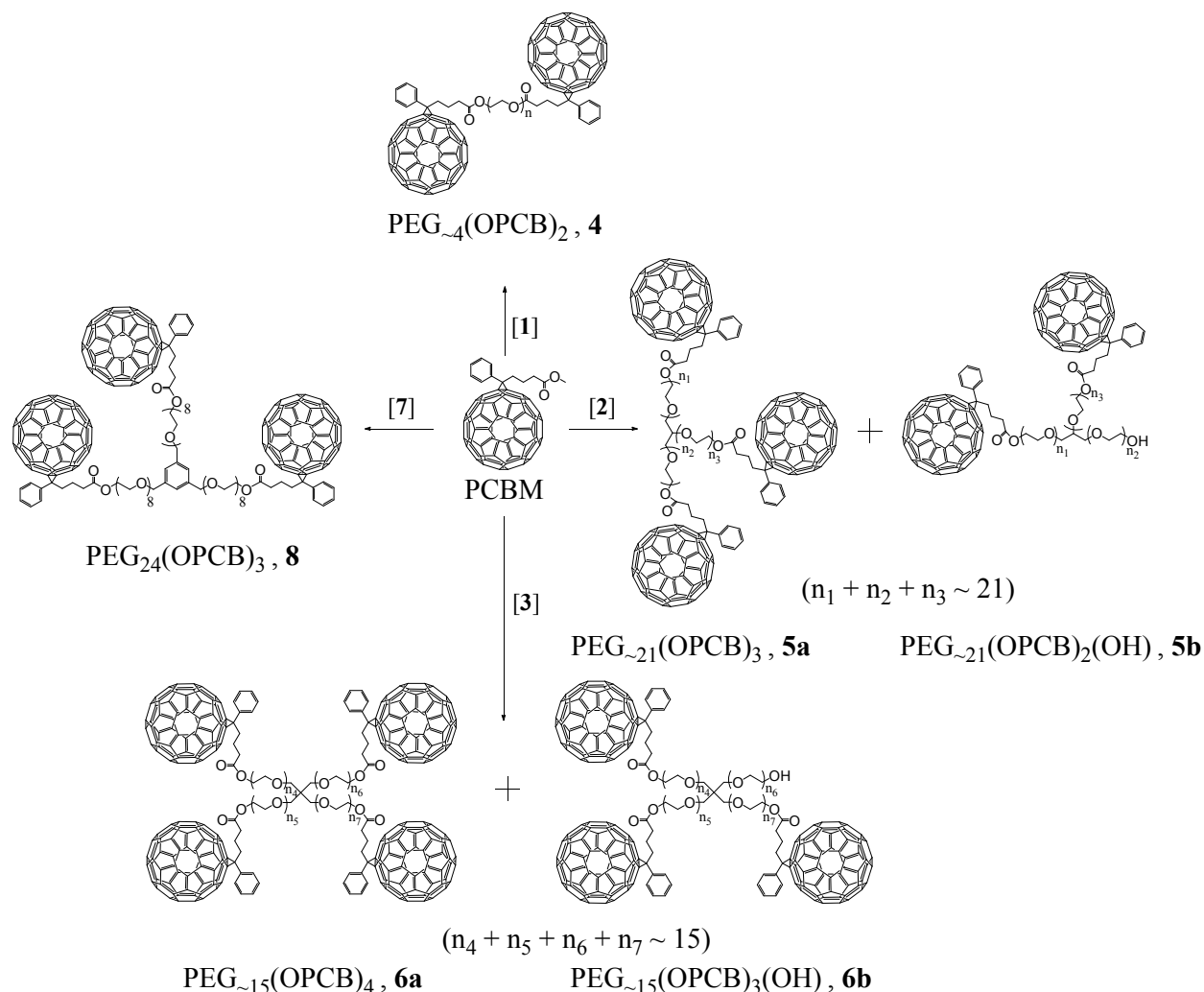
433, 510 nm; m/z (MALDI-TOF) calc'd for $[\text{C}_{319}\text{H}_{112}\text{O}_{23}\text{Na}]^+$ 4331.75 m/z , found $[\text{M}+\text{Na}]^+$ 4332.85 m/z .

Synthesis of PEG₂₄(OPCB)₃, **8**.

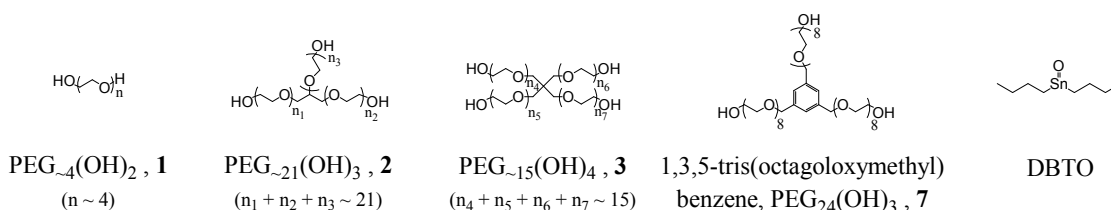
Monodisperse tris-C₆₀ 3-arm branched PEG **8** was synthesized from PEG₂₄(OH)₃ (**7**, 25 mg, 0.02 mmol), PCBM (60 mg, 0.06 mmol) and DBTO (1.6 mg, 0.007 mmol) using the general method described above, and fractionated through silica gel columns (2 ×), followed by preparative TLC (3 ×), eluting with toluene-methanol (9:1 v/v), to give PEG₂₄(OPCB)₃ (**8**, 4 mg, 5 %) as a brown solid. R_f toluene-methanol (9:1 v/v) 0.35; δ_{H} (400 MHz, CDCl₃) 2.21 (quin, $J = 8.1$ Hz, 6H), 2.57 (t, $J = 7.5$ Hz, 6H), 2.93 (t, $J = 8.1$ Hz, 6H), 3.61-3.76 (m, 96H), 4.25 (t, $J = 4.3$ Hz, 6H), 4.56 (s, 6H), 7.25 (s, 3H), 7.51 (t, $J = 7.5$ Hz, 3H), 7.57 (t, $J = 7.6$ Hz, 6H), 7.94 (d, $J = 7.9$ Hz, 6H); ν (FT-IR; ATR) 2922 (aliphatic **C-H** stretching), 2852 (aliphatic **C-H** stretching), 1728 (carbonyl stretching of PCBM ester), 1462, 1378, 1265 (**C-C** stretching in fullerene), 1079 (**C-O** symmetric stretching of PEG), 1045, 889, 722 cm^{-1} ; m/z (MALDI-TOF) calc'd for $[\text{C}_{270}\text{H}_{138}\text{O}_{30}\text{Na}]^+$ 3881.92 m/z , found $[\text{M}+\text{Na}]^+$ 3881.83 m/z .

Results and discussion

Multifullerene-end-capped PEGs, PEG₋₄(OPCB)₂ (**4**), PEG₋₂₁(OPCB)₃ (**5a**), PEG₋₁₅(OPCB)₄ (**6a**) and PEG₂₄(OPCB)₃ (**8**) were synthesized via a one-step transesterification of PCBM with the corresponding hydroxyl-terminated PEG derivatives [polydisperse PEG(OH)_{*n*} **1-3**, and monodisperse PEG₂₄(OH)₃ **7**] in the presence of a catalytic amount of dibutyltin oxide (DBTO), at 140°C in dry *ortho*-dichlorobenzene (*o*-DCB) (Scheme 1).²⁹ Small aliquots from the crude reaction mixture were analysed after 2h, and then every 24h, up to 5 days by ¹H NMR. ¹H NMR analysis (see Supporting Information, *Figure S1*) showed the appearance and growth of a new triplet signal at 4.25 ppm corresponding to the newly formed methylene ester protons (**-CH₂-O-C=O**).²¹ The signal intensity increased significantly during the first three days, after which point growth slowed, indicating that the transesterification reaction could proceed no further. As no pure mono-disperse PEG_{*n*}(OH)_{3/4} (**2** or **3**) were commercially available, the study commenced with polydisperse PEG₋₄(OH)₂ (**1**, average molecular weight $M_n \sim 200$ manufacturer value; $M_n = 203$ from NMR (see below)), PEG₋₂₁(OH)₃ (**2**, average $M_n \sim 1000$ manufacturer value; $M_n = 1029$ from NMR) and PEG₋₁₅(OH)₄ (**3**, average $M_n \sim 797$ manufacturer value; $M_n = 786$ from NMR). After azeotropic drying with acetonitrile,



Reaction condition : 1.1 eq PCBM per OH, 0.11 eq DBTO per OH, *o*-DCB, 140°C, N₂, 5 days



Scheme 1. The transesterification of PCBM with PEG_x(OH)_n (1-3) and PEG₂₄(OH)₃ (7) to yield polydisperse PEG_x(OPCB)_n (4-6) and monodisperse PEG₂₄(OPCB)₃ (8).

these cores were used for the preparation of PEG₄(OPCB)₂ (4), PEG_{~21}(OPCB)₃ (5a), and PEG_{~15}(OPCB)₄ (6a), respectively, and the resulting compounds were purified by column and/or preparative thin layer chromatography (TLC). MALDI-TOF mass spectral analysis, supported by ¹H NMR, FTIR and UV-vis techniques, were used for characterization of the phenyl-C₆₁-butyryl (PCB)-functionalised PEGs.

The extent of the transesterification reaction can be determined by the ratio of the chain terminal proton resonances to the polymeric backbone. However, the resonances at around 3.7

ppm corresponding to methylene (alpha proton, α) bearing the terminal hydroxyl groups overlap with the PEG backbone. To establish a suitable control and confirm the nature of starting materials, each starting PEG_x(OH)_n was treated with highly reactive trifluoroacetic anhydride (TFAA)-CDCl₃ (1:19 v/v) in an NMR tube to give the corresponding per-acylated PEG_n(OCOCF₃)_n derivative *in situ*.³¹ The electronegative trifluoroacetyl substituent deshields the adjacent acyloxymethylene protons (alpha proton, α), F₃CCO₂CH₂CH₂O, giving a signal at *ca.* 4.51 ppm well

resolved from the PEG backbone. Thus, the average number of repeating units of each PEG compound was obtained from the integral ratio of the acyloxymethylene protons to the main PEG signals (see supporting information, *Figure S3-5*), and found to be 4, 21 & 15 for bis-OH, tris-OH and tetrakis-OH terminated PEGs respectively. These ^1H NMR findings are consistent with the number average of molecular weight distributions in the MALDI spectra of the pure PEG cores (supporting information, *Figure S8-9*). The ^1H NMR of $\text{PEG}_{-15}(\text{OCOCF}_3)_4$ (supporting information, *Figure S5*) indicated that the tetrakis-OH terminated PEG contains a distinctive second variant; most likely a fraction of the mixture has a $\text{CH}_2\text{-OH}$ stub directly linked to the central sp^3 carbon, rather than through an ether linkage, i.e. in **3**, one of $n_{4/5/6/7} = 0$; (see *ESI* for detailed characterisation). Since PCBM is a bulky molecule, a relatively longer side chain should assist the grafting reaction; steric effects may prevent fullerene attaching onto short side chains, particularly onto the CH_2OH stub.

The MALDI-TOF mass spectrum of $\text{PEG}_{-4}(\text{OPCB})_2$ (**4**) (Figure 1A) verified the formation of doubly transesterified $\text{PEG}_{-4}(\text{OH})_2$, showing four main clusters of positively charged $[\text{M}+\text{Na}]^+$ ions ranging from m/z 1970 to 2160, where each peak region corresponds to the bis-fullerene end-capped PEG dumbbells with between 4 and 7 ethylene oxide repeat units. (See Supporting Information, *Figure S10* for the full MALDI-TOF mass spectrum of **4**; no mono-fullerene substituted species is visible). Considering the penta-ethylene oxide repeat unit cluster in detail (Figure 1A*, upper), the experimental isotopic peak pattern of $\text{PEG}_{-4}(\text{OPCB})_2$ (**4**) was consistent with the simulated pattern (Figure 1A*, lower) across all expected masses, $[\text{M}+\text{Na}]^+_{\text{obs}} = 2017.23$, $[\text{M}+\text{Na}]^+_{\text{calc}} = 2017.21$. In the IR spectrum of **4** (Figure 2b), there is no OH stretch at around 3500 cm^{-1} , indicating that there very little, if any mono-fullerene substituted PEG_{-4} in the product fraction. In the ^1H NMR spectrum of $\text{PEG}_{-4}(\text{OPCB})_2$ (Supporting information, *Figure S11*), a new triplet at 4.25 ppm indicates the successful acylation of the linear PEG. The observed integral ratio between the newly formed acyloxymethylene resonance (alpha protons) and the main PEG signal was 1:4.25, whereas the ratio observed in fully trifluoroacetylated linear PEG was 1:3.25. Rather than incomplete reaction, the IR evidence suggests that this shift in ratio is more likely to arise due to the preferential double reaction of the longer PEG chains, because of steric constraints on the second fullerene addition. From the observed integral ratio, the as produced dumbbell derived under these conditions contains an average of 5 repeating units whereas the starting $\text{PEG}_{-4}(\text{OH})_2$ has an average of 4 repeating units.

The purifications of all bis-, tris- and tetrakis-fullerene adducts were performed by multiple rounds of column chromatography and preparative TLC. Since PEGs bearing unreacted hydroxyl groups have a stronger affinity for silica gel, any remaining partially unreacted PEG is eluted in the later fractions. The polarity of the molecules decreases with increasing number of covalently grafted non-polar fullerenes. Hence, the most highly substituted adducts are collected in the first fraction to elute using Tol/MeOH 9:1 v/v. All detailed analyses were carried out with these initially eluted chromatographic fractions.

Tris-fullerene substituted PEG

The MALDI spectrum of **5** (supporting information, *Figure S13*) clearly confirms the successful formation of the tris-fullerene polymer (mean peak distribution at $\sim 3630\text{ m/z}$). The observed monoisotopic mass of tris-fullerene substituted 3-arm PEG (with 20 repeating units) (Figure 1B*) appeared to be shifted by 2 m/z to lower mass, most likely due to the limit of spectrometer sensitivity. The overall shape of the monoisotopic mass reassembled that of the calculated value for the tris-fullerene substituted 3-arm PEG. However, two other peak distributions (mean peak distribution at around 2750 and 1740 m/z) were also observed. Since the transesterification of fullerene and PEG hydroxyls is a sequential reaction, mono- and bis-fullerene substituted PEGs may be present along with the desired tris-fullerene adduct. In order to identify the origin of the peaks in the MALDI-TOF spectrum, each peak distribution corresponding to tris- and possible mono- and bis-fullerene PEG distributions were compared with that of the starting PEG (*Figure S14(top)*). Both tris- and bis-substituted species had an average of 20 repeating units (mean peak distribution at around 3630 and 2750 m/z respectively), but the mono-substituted PEG peak had a mean peak distribution at around 1740 m/z , corresponding to an average of 17 repeating units. The expected mono-substituted 3-arm PEG would have an average of 20 repeating units with a mean peak distribution at around 1880 m/z ; the difference of 3 repeating units between the observed mono-substituted species and the bis/tris substituted PEG star suggests that the mono-substituted distribution at 1740 m/z may result from fragmentation of the bis/tris PEG stars. An alternative explanation is that the shorter mono-fullerene substituted 3-arm PEG is less polar and eluted preferentially with the more substituted products; however, the change in length would be expected to be less significant than the change in the number of available hydroxyls. The high polydispersity of the fullerene end-capped PEG adducts $\text{PEG}_{-21}(\text{OPCB})_3$ (**5a**) made chromatographic

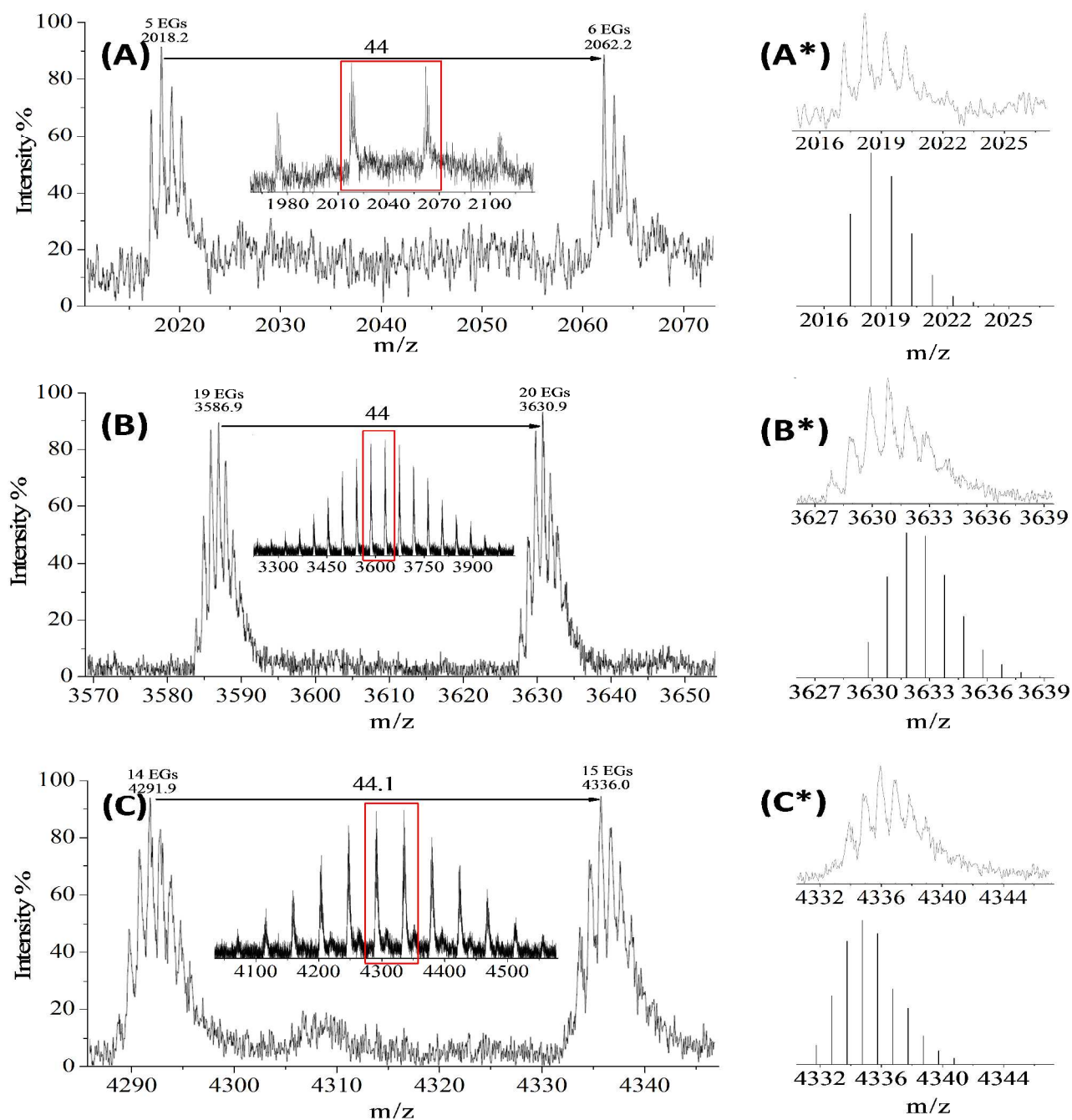


Figure 1. Experimental and simulated MALDI-TOF mass spectra of $[\text{PEG}(\text{OPCB})_n+\text{Na}]^+$ (**4-6**) confirming successful transesterification of PCBM with polydisperse PEGs **1-3**: (A) $\text{PEG}_{-4}(\text{OPCB})_2$ (**4**); (B) $\text{PEG}_{-21}(\text{OPCB})_3$ (**5**); (C) $\text{PEG}_{-15}(\text{OPCB})_4$ (**6**). The full spectra are given in the Supporting Information. For each of **4-6**, the whole product cluster (inset) is expanded (red rectangle \rightarrow large image) to show the PEG monomer spacing, and further expanded (**A***, $n = 5$; **B***, $n = 20$; and **C***, $n = 15$) to show the monoisotopic peak pattern (top), with comparison to the corresponding simulated peak pattern (below).

purification of very difficult; the variations in PEG molecular weight and degree of fullerene substitution smeared the variation in polarity. Hence, further efforts were made to isolate $\text{PEG}_{-21}(\text{OPCB})_3$ (**5a**) from its mixture by repeated column chromatography, and multiple preparative TLC (up to 3 times). However, the purity did not improve significantly despite these lengthy steps. The signal intensity ratio of the bis- and tris-

fullerene distribution in MALDI improved only to about 84:16 from 90:10 after initial work-up. As the MALDI signal intensity may not always reflect molecular abundance, the ratio was also determined from the ^1H NMR integral (Figure S12). In the case of $\text{PEG}_{-21}(\text{OCOCF}_3)_3$, the ratio of chain terminal to backbone signals was 6:84 (confirming 21 ethylene oxide units per dendrimer molecule, as noted above). For the fullerene end-

capped 3-arm dendrimer **5**, the butyryl peaks of the PCB moiety and the acyloxymethylene of the chain termini are also well resolved from the polymeric PEG peak, and the corresponding ratio of fullerene ends to backbone signals was 4.4:85.6. Assuming that the product is a mixture of only PEG₋₂₁(OPCB)₂(OH) [**5b**] and PEG₋₂₁(OPCB)₃ [**5a**], (i.e. that the mono-fullerene substituted PEG star signal in MALDI-TOF spectrum is due to fragmentation) the best fit for the α -proton integration indicates a 90:10 ratio of PEG₋₂₁(OPCB)₂(OH) [**5b**] to PEG₋₂₁(OPCB)₃ [**5a**], a value comparable to the ratio derived from the MALDI peak intensities (84:16).

Tetrakis-fullerene substituted PEG

The MALDI-TOF spectra of PEG₋₁₅(OPCB)₄ [**6a**] and PEG₋₁₅(OPCB)₃(OH) [**6b**] exhibited similar distribution patterns to the tris-fullerene substituted PEG, but with different masses, having mean peak distributions around 4330 and 3410 m/z respectively (See supporting information, *Figure S16*). The observed monoisotopic mass of the tetrakis-fullerene substituted 4-arm PEG (Figure 1C*) appeared to be shifted by 2 m/z but resembled the shape of the calculated monoisotopic mass (with 15 repeating units). Within the limits of the spectrometer sensitivity, the result confirmed the formation of the desired PEG₋₁₅(OPCB)₄ [**6a**]. Similar to the synthesis of PEG₋₂₁(OPCB)₃ [**5a**], the incompletely substituted 4-arm PEG, PEG₋₁₅(OPCB)₃(OH) [**6b**] was also observed in the spectrum at around 3410 m/z. An additional mass distribution corresponding to the possible bis-fullerene substituted adduct was also observed at around 2240 m/z. However, detailed comparison (see supporting information, *Figure S17*) indicates that only the tris- and tetrakis-fullerene derivatives are likely to be primary signals. The tris- and tetrakis-fullerene distribution both have an average of 15 repeating units, whereas the bis-fullerene distribution was found to have an average of 8 repeating units. MALDI-TOF spectra of the starting 4-arm PEG (Figure S9) showed no evidence of any 8 repeating unit fraction within the polymer. Therefore, it is clear that the peak distribution at around 2240 m/z in the tetrakis-fullerene substituted PEG spectra resulted from fragmentation of the higher mass species. Whilst the MALDI-TOF indicated a 50:50 ratio between the tris- and tetrakis-fullerene signal intensities (Figure S16), the NMR integral ratios provided a more reliable measure. The integral ratio of α -protons versus the main PEG backbone protons for fully acylated PEG₋₁₅(OCOCH₃)₄ was 8:60 (See Figure S5). The observed ratio of the corresponding tris- and tetrakis-fullerene substituted PEG star in the ¹H NMR of mixture of [**6a**, **6b**] was 7.5:60.5 (See Figure S15). Assuming that, as shown in the MALDI-TOF analysis, the NMR integration solely results from the contribution of tris- and tetrakis- substituted PEG₋₁₅ stars, the best fit to the α -proton integration is a 1:1 ratio of PEG₋₁₅(OPCB)₃(OH) [**6b**] to PEG₋₁₅(OPCB)₄ [**6a**]. As in the case of PEG₋₂₁(OPCB)₃ (**5a**), extensive purification could not separate the species with

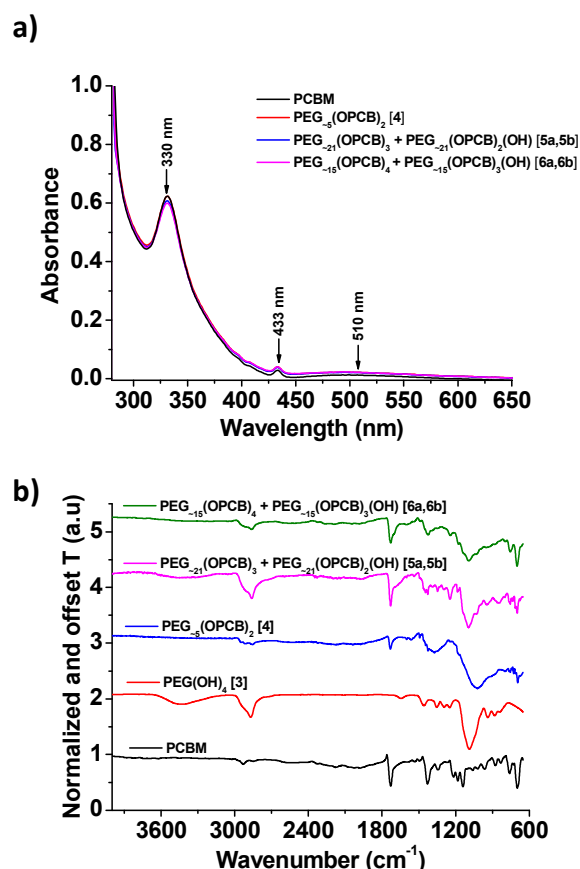


Figure 2. Photospectrometric data for PCB-capped PEG dendrimers: **a)** UV-vis spectra of PCBM, PEG₋₄(OPCB)₂ (**4**), PEG₋₂₁(OPCB)₃ & PEG₋₂₁(OPCB)₂(OH) (**5a** and **5b**), and PEG₋₁₅(OPCB)₄ & PEG₋₁₅(OPCB)₃(OH) (**6a** and **6b**) recorded in toluene. Each concentration was adjusted to around Abs_{330 nm} ~0.6 for ease of comparison; **b)** FTIR spectra of PCBM, PEG₋₁₅(OH)₄ (**3**), PEG₋₄(OPCB)₂ (**4**), PEG₋₂₁(OPCB)₃ (**5**) and PEG₋₁₅(OPCB)₄ (**6**).

differing degrees of fullerene substitution, presumably due to the level of PEG polydispersity.

Higher molecular mass species tend to be harder to ionise in MS and therefore peak intensity is not generally used in determination of natural abundance.³² However, considering the calculation based on the NMR peak integral, the values derived from both MALDI and NMR are very comparable. Although NMR integration is more reliable for determination of actual abundance, it seems that MALDI peak intensity may also be used as a good approximation in the current system.

The UV-vis spectra of PEG₋₄(OPCB)₂ (**4**), PEG₋₂₁(OPCB)₃ (**5**) and PEG₋₁₅(OPCB)₄ (**6**) products in toluene have three electronic absorption bands at 330, 433 and 510 nm (Figure 2a), similar to PCBM, as expected. The retention of the optoelectronic properties should be helpful for PV applications. The starting PEG(OH)_n (**1-3**) do not contribute to the absorbance (see Supplementary Information *Figure S18* for UV-vis spectra of **1-3**).²³ However, in FTIR (Figure 2b), the intensity of the -OH stretching bands at around 3400 cm⁻¹ were significantly reduced in all products indicating successful transesterification. The -OH bands did not disappear completely in 3-arm **5** and 4-arm **6** as the substituted PEG still

contained a small proportion of free terminal hydroxyl groups. As in previous reports,^{21, 23} no spectral change was observed for the bands at 1732 cm⁻¹ (carbonyl stretching of PCB-PEG ester), 1180 cm⁻¹ and 1430 cm⁻¹ (C-C & C=C stretching in fullerene) and 1095 cm⁻¹ (C-O symmetric stretching of PEG) compared to the spectra of pure PCB and PEG₋₁₅(OH)₄ [3] (Figure 2b).

The MALDI-TOF results together with NMR, FTIR and UV-vis data confirmed the synthesis of multi-fullerene end-capped PEG dumbbells PEG₄(OPCB)₂ [4] and stars PEG₂₁(OPCB)₃ [5a] and PEG₁₅(OPCB)₄ [6a], through the transesterification of PCB using polydisperse PEGs starting materials. However, the polydispersity, particularly of the tris and tetrakis fullerene products remained problematic. To synthesise monodisperse multi-fullerene end-capped PEG stars, a monodisperse PEG core was required. PEG₂₄(OH)₃ [7] was synthesized following a recent procedure;³⁰ NMR and MALDI-TOF. (see supporting information, *Figure S19, S20 and S21* for ¹H, ¹³C NMR and MALDI-TOF spectra of PEG₂₄(OH)₃ [7]) confirmed the monodispersed nature of the starting material, with a mass of 1247.7 Da. This star-shaped PEG, PEG₂₄(OH)₃ [7] was then transesterified with PCB using the same procedure described above for PEG_x(OH)_n [1-3]. Due to the monodisperse character of PEG₂₄(OH)₃ [7], it was possible to separate the resulting monodisperse tris-fullerene end-capped PEG, PEG₂₄(OPCB)₃ [8] from the mixture of mono- and bis-fullerene end-capped PEG₂₄(OPCB)_x(OH)_y employing two rounds of column chromatography, followed by three rounds of preparative thin layer chromatography. Since this same purification protocol had failed to isolate the pure materials from the earlier crude product mixtures, it is clear that the monodispersity of the PEG star is helpful in differentiating the products, although the separation is still lengthy.

Monodisperse PEG₂₄(OPCB)₃ [8]

The MALDI-TOF spectrum of isolated PEG₂₄(OPCB)₃ [8] (Figure 3) showed the expected monoisotopic mass at 3881.82 Da, close to the calculated value of 3881.91 Da (Figure 3D*). The mass spectrometric results were further supported by the ¹H NMR spectrum which displayed a new triplet signal corresponding to the acyloxymethylene protons (-CH₂-O-C=O) adjacent to the newly formed ester carbonyl, at 4.25 ppm (see Figure 4). The starting material PEG₂₄(OH)₃ [7] has three arms, each having eight ethylene oxide repeating units (96 protons in total). After transesterification, one would expect six of 96 protons to be converted into acyloxymethylene protons (d), resolving them from the large backbone resonance. The hydroxyl protons of PEG₂₄(OH)₃ [7] at 3.15 ppm (see supporting information, *Figure S19*) disappeared after transesterification, and the integrals ratios of the acyloxymethylene (labelled as d in Figure 4) to the PEG backbone (labelled as CH₂CH₂O in Figure 4) protons was found to be 6.0:90.4 (consistent with the expected 6:90 for complete acylation). Both MALDI-TOF and ¹H NMR analysis provide strong evidence for the successful formation

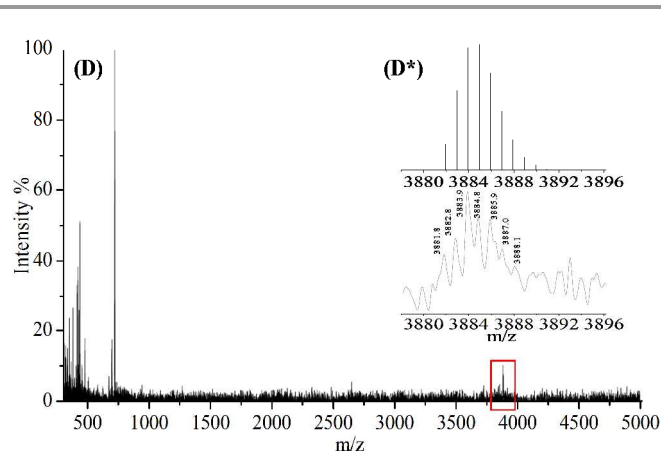


Figure 3. Experimental and theoretical MALDI-TOF spectra confirming successful transesterification of PCB with PEG₂₄(OH)₃ [7]. Full MALDI-TOF mass spectrum of PEG₂₄(OPCB)₃ [8] (D). Expanded region (represented by rectangle) shows the monoisotopic peak pattern of PEG₂₄(OPCB)₃ [8] (bottom D*). Theoretically simulated peak pattern (upper D*) for PEG₂₄(OPCB)₃ [8]. The signal at 720 m/z was attributed to C₆₀ and below 720 m/z features predominantly related to matrix DCTB

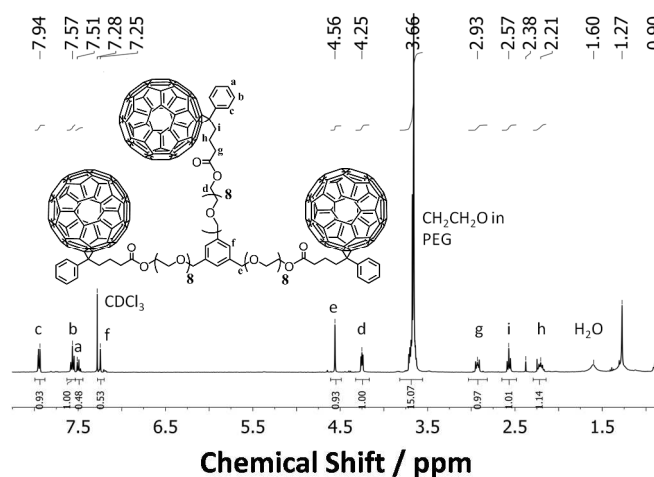


Figure 4. ¹H NMR spectrum of pure monodisperse PEG₂₄(OPCB)₃ [8]. Integration of 1 unit = 6 H. Trace amounts of water (1.60 ppm) and vacuum grease (1.27 and 0.90 ppm) were observed.

and isolation of the desired monodispersed tris-fullerene substituted PEG₂₄(OPCB)₃ [8].

Due to the difficulty in purification, only the fractions containing the desired species were separated and studied closely. During column chromatography a large coloured fraction remained visible in the column. From the analysis of the primary fractions, the remaining materials in the column are likely to be species with lower degrees of substitution. Similar to the preparation of 3-arm adducts of oligothiophenevinyls and C₆₀,³³ the yield of isolated PEG₂₄(OPCB)₃ [8] and all other adducts were low, even though the reaction medium was saturated with PCB.²⁹ The final yields of fully substituted products were 4 % for PEG₂₁(OPCB)₃ [5], 8 % for PEG₁₅(OPCB)₄ [6] and 5 % for PEG₂₄(OPCB)₃ [8]. In the case of PEG₁₅(OPCB)₄ [6], the presence of a minor 3-arm PEG

impurity in the starting material may have affected the overall yield of the reaction. Due to the small yields, elemental analyses were not performed. An initial NMR integration study (Figure S1) of the α -protons (adjacent to newly formed ester) revealed that the reaction proceeded slowly (about 3 days), after which time the catalyst may have become deactivated. Furthermore, although the reaction was carried out at 140 °C, well above the boiling point of methanol, it is possible that the trace amount of methanol released by transesterification may have allowed the reverse reaction to occur to some extent. Finally, although the reaction was kept under nitrogen throughout, the work-up and column chromatography were performed in air. It is well documented that fullerene is a good photo-sensitizer which could easily convert molecular oxygen into singlet oxygen. Fullerene oxidises and/or polymerises in the presence of singlet oxygen, limiting its solubility and that of its adducts.³⁴ Therefore, polymerisation of the initially produced fullerene end-capped PEGs during purification may have significantly limited the final purified yield.

Conclusions

Multiple fullerene end-capped PEGs were synthesized for the first time using single step transesterification of PCBM with PEGs. The monodisperse nature of PEG₂₄(OH)₃ [7] allowed isolation of the pure monodisperse fullerene end-capped PEG star PEG₂₄(OPCB)₃ [8] from the crude reaction mixture. Monodisperse PEGs with multiple fullerene arms are attractive for BHJ solar cells. It may be possible to tune the phase segregation and/or self-assembly of the fullerene-grafted PEGs by controlling the length of the starting PEG chains and the number of attached fullerene species, whilst retaining the optoelectronic character of PCBM. The synthetic procedure could be applied to the synthesis of other monodisperse multi-arm species with higher mass fullerenes (C₇₀/C₈₂) as experimental data suggest that higher PV efficiency may be achieved in this way.³⁵ Such fullerene adducts are also not necessarily limited to a PEG core. Since the reaction relies on converting the hydroxyl into an ester, any cores with terminal OH groups could be used. The observed partial fullerene substitution of the 3/4-armed products is likely related to the low reaction yields, though steric effects related to short PEG arms may also have played a role. The reaction yield (and likely degree of substitution) might be increased by adjusting the catalyst system, or by using initial fullerene derivatives bearing a more reactive ester (e.g. pentafluorophenyl ester). Future applications of well-defined multiple fullerene stars are likely to emerge with wider availability of well-characterised monodisperse materials. Fullerene dyads have become a popular topic in PV applications. This synthetic procedure for well-defined fullerene derivatives may offer new opportunities for the future study of multiple fullerenes adducts, especially when a conjugated polymer is employed in the synthesis, in place of PEG.

Acknowledgements

The authors would like to commemorate the late Dr. Joachim H. G. Steinke (1964-2013) for his contribution to this work and to the polymer chemistry field. We acknowledge the EPSRC UK National Mass Spectrometry Service at Swansea and EPSRC research grant EP/G007314/1. MKB is particularly grateful to the Scientific and Technological Research Council of Turkey (TUBITAK) for post-doctoral research permission.

Notes

^a Department of Chemistry, South Kensington Campus, Imperial College London, London, SW7 2AZ, UK.

^b Department of Chemical Engineering, University College London, London, WC1E 6BT, UK

^c Department of Chemical Engineering, South Kensington Campus, Imperial College London, London, SW7 2AZ, UK.

† These authors contributed equally to this work

Electronic Supplementary Information (ESI) available: [NMR spectra, and MALDI-TOF spectra of the polydisperse multifullerene PEG adducts]. See DOI: 10.1039/b000000x/

References

1. A. Dodabalapur, H. E. Katz, L. Torsi and R. C. Haddon, *Science*, 1995, 269, 1560-1562.
2. R. C. Haddon, T. Siegrist, R. M. Fleming, P. M. Bridenbaugh and R. A. Laudise, *Journal of Materials Chemistry*, 1995, 5, 1719-1724.
3. G. Yu, J. Gao, J. C. Hummelen, F. Wudl and A. J. Heeger, *Science*, 1995, 270, 1789-1791.
4. L. S. Roman, M. R. Andersson, T. Yohannes and O. Inganas, *Advanced Materials*, 1997, 9, 1164-1168.
5. L. Garlaschelli, D. Pasini and F. Spaggiari, *European Journal of Organic Chemistry*, 2005, DOI: 10.1002/ejoc.200500224, 4322-4327.
6. Y. H. Zhu, S. Bahnmüller, C. B. Ching, K. Carpenter, N. S. Hosmane and J. A. Maguire, *Tetrahedron Letters*, 2003, 44, 5473-5476.
7. M. Carano, C. Corvaja, L. Garlaschelli, M. Maggini, M. Marcaccio, F. Paolucci, D. Pasini, P. P. Righetti, E. Sartori and A. Toffoletti, *European Journal of Organic Chemistry*, 2003, 374-384.
8. M. Svensson, F. L. Zhang, S. C. Veenstra, W. J. H. Verhees, J. C. Hummelen, J. M. Kroon, O. Inganas and M. R. Andersson, *Advanced Materials*, 2003, 15, 988-991.
9. I. A. Howard, R. Mauer, M. Meister and F. Laquai, *Journal of the American Chemical Society*, 2010, 132, 14866-14876.
10. C.-H. Hsieh, Y.-J. Cheng, P.-J. Li, C.-H. Chen, M. Dubosc, R.-M. Liang and C.-S. Hsu, *Journal of the American Chemical Society*, 2010, 132, 4887-4893.
11. G. W. Wang, T. H. Zhang, E. H. Hao, L. J. Jiao, Y. Murata and K. Komatsu, *Tetrahedron*, 2003, 59, 55-60.
12. M. Reyes-Reyes, K. Kim and D. L. Carroll, *Applied Physics Letters*, 2005, 87, 083506.
13. F. Lincker, P. Bourgun, H. Stoeckli-Evans, I. M. Saez, J. W. Goodby and R. Deschenaux, *Chemical Communications*, 2010, 46, 7522-7524.
14. H. Xin, G. Ren, F. S. Kim and S. A. Jenekhe, *Chemistry of Materials*, 2008, 20, 6199-6207.
15. S. M. Tuladhar, M. Sims, S. A. Choulis, C. B. Nielsen, W. N. George, J. H. G. Steinke, D. D. C. Bradley and J. Nelson, *Organic Electronics*, 2009, 10, 562-567.
16. C. M. Björström, K. O. Magnusson and E. Moons, *Synthetic Metals*, 2005, 152, 109-112.
17. P. W. M. Blom, V. D. Mihaileti, L. J. A. Koster and D. E. Markov, *Advanced Materials*, 2007, 19, 1551-1566.

18. M. Campoy-Quiles, T. Ferenczi, T. Agostinelli, P. G. Etchegoin, Y. Kim, T. D. Anthopoulos, P. N. Stavrinou, D. D. C. Bradley and J. Nelson, *Nature Materials*, 2008, 7, 158-164.
19. H. Hoppe and N. S. Sariciftci, *Journal of Materials Research*, 2004, 19, 1924-1945.
20. C. Müller, T. A. M. Ferenczi, M. Campoy-Quiles, J. M. Frost, D. D. C. Bradley, P. Smith, N. Stingelin-Stutzmann and J. Nelson, *Advanced Materials*, 2008, 20, 3510-3515.
21. J. W. Jung, J. W. Jo and W. H. Jo, *Advanced Materials*, 2011, 23, 1782-1787.
22. J.-Y. Jeng, M.-W. Lin, Y.-J. Hsu, T.-C. Wen and T.-F. Guo, *Advanced Energy Materials*, 2011, 1, 1192-1198.
23. Q. Tai, J. Li, Z. Liu, Z. Sun, X. Zhao and F. Yan, *Journal of Materials Chemistry*, 2011, 21, 6848-6853.
24. T. Song, S. H. Goh and S. Y. Lee, *Polymer*, 2003, 44, 2563-2567.
25. D. Taton, S. Angot, Y. Gnanou, E. Wolert, S. Setz and R. Duran, *Macromolecules*, 1998, 31, 6030-6033.
26. H. C. Yau, M. K. Bayazit, J. H. G. Steinke and M. S. P. Shaffer, *Macromolecules*, 2014, 47, 4870-4875.
27. M. Graetzel, R. A. J. Janssen, D. B. Mitzi and E. H. Sargent, *Nature*, 2012, 488, 304-312.
28. Q. Wei, T. Nishizawa, K. Tajima and K. Hashimoto, *Advanced Materials*, 2008, 20, 2211-2216.
29. J. C. Hummelen, F. B. Kooistra and D. F. Kronholm, *USPATENT*, 2005, US2005245606.
30. G. Szekely, M. Schaepertoens, P. R. J. Gaffney and A. G. Livingston, *Polym. Chem.*, 2014, 5, 694-697.
31. M. Tryznowski, K. Tomczyk, Z. Frasz, J. Gregorowicz, G. Rokicki, E. Wawrzynska and P. G. Parzuchowski, *Macromolecules*, 2012, 45, 6819-6829.
32. G. Montaudo, F. Samperi and M. S. Montaudo, *Progress in Polymer Science*, 2006, 31, 277-357.
33. C. Martineau, P. Blanchard, D. Rondeau, J. Delaunay and J. Roncali, *Advanced Materials*, 2002, 14, 283-287.
34. H. Watanabe, E. Matsui, Y. Ishiyama and M. Senna, *Tetrahedron Letters*, 2007, 48, 8132-8137.
35. X. Meng, W. Zhang, Z. a. Tan, Y. Li, Y. Ma, T. Wang, L. Jiang, C. Shu and C. Wang, *Advanced Functional Materials*, 2012, 22, 2187-2193.

